# Effective-mass theory of metal-semiconductor contact resistivity

Walter A. Harrison, Andreas Goebel, and Paul A. Clifton

Citation: Applied Physics Letters **103**, 081605 (2013); doi: 10.1063/1.4818265
View online: http://dx.doi.org/10.1063/1.4818265
View Table of Contents: http://scitation.aip.org/content/aip/journal/apl/103/8?ver=pdfcov
Published by the AIP Publishing



# Effective-mass theory of metal-semiconductor contact resistivity

Walter A. Harrison,[1,2,a)] Andreas Goebel,[1] and Paul A. Clifton[1]
[1]*Acorn Technologies, Inc., Palo Alto, California 94306, USA*
[2]*Department of Applied Physics, Stanford University, Stanford, California 94305, USA*

(Received 4 June 2013; accepted 23 July 2013; published online 20 August 2013)

We have calculated the contact resistivity for a metal-silicon interface, using an accurate application of effective-mass theory that includes tunneling and quantum reflection. We found that earlier treatments missed an increase in resistivity of a factor of ten due to the mismatch of the wavefunctions at the interface, not included in the WKB approximation. This arises in effective-mass theory for all metal-semiconductor interfaces. We carried out full numerical calculations of the interface resistivity and describe approximations which lead to explicit formulae for the current flow, allowing one to see the dependence of the resistivity on doping, Schottky-barrier height, temperature, crystal orientation, and choice of metal. Finally, we see how the number and energy distribution of transmitted carriers changes as a function of doping density. © *2013 AIP Publishing LLC*.
[http://dx.doi.org/10.1063/1.4818265]

Schottky barriers at metal-semiconductor interfaces have been investigated since early on[1,2] and are still an area of active and broad scientific investigation.[3] Technologically, the shrinking area of the metal-semiconductor contacts in silicon CMOS integrated circuits drives the need for a lower specific contact resistivity $\rho_c$.[4] Reducing Schottky barrier heights much below their natural "pinned" value is an important contribution to reducing $\rho_c$.[5–8] Early theoretical treatment employing an effective-mass description of the semiconductor bands[9] led to piece-wise approximations widely used in silicon engineering,[10] even though Yu's Eq. (2) in Ref. 10 for $R_c$ at high doping ($N_d > 10^{20}\,\mathrm{cm}^{-3}$) is not valid for small barriers (<0.5 eV.) Quantum mechanical reflection (QMR), the temperature and doping dependence of the effective-mass, and the tensor-like properties of the effective-mass have been investigated previously.[11–13] Given the recent interest, we have developed a unified physics-based model that remains appropriate for low barrier heights, does not require any division of the problem into separate models for different conduction regimes, and includes a more appropriate treatment of QMR at the metal-semiconductor interface.

In this paper, we treat the case of electron transport across a Schottky barrier at a (100) metal-silicon interface as shown in Fig. 1 for heavy doping, though for lighter doping the Fermi energy will drop below the conduction-band minimum. As in Refs. 9 and 10 we assume a barrier height and shape and go on to derive the interface resistivity for the given case. Our treatment covers the range from very low to very high doping densities, small to large Schottky barriers, includes temperature dependence, and takes the metal band structure into account by evaluating the size of the metal Fermi wavevector.

The electron current is calculated around zero bias by multiplying the electron impingement rate at the interface with their transmission probability $Tr$ and integrating over all states on one side, then subtracting the reverse flow with the Fermi energy on the other side shifted by $\Delta V$

$$J = \frac{1}{A}\frac{2LA}{(2\pi)^3}\int dk_\parallel 2\pi dk_\perp \frac{e}{\hbar L}\frac{\partial \varepsilon_\parallel}{\partial k_\parallel} \times Tr(\varepsilon_\parallel, \varepsilon_\perp)\frac{\partial f_0[(\varepsilon_\parallel + \varepsilon_\perp - \varepsilon_F)/kT]}{\partial \varepsilon_F}\Delta V. \quad (1)$$

The integrals are converted to integrals over kinetic energies $\varepsilon_\parallel$ and $\varepsilon_\perp$ in the semiconductor parallel and perpendicular to the current flow along the $x$-direction, respectively. The integral over perpendicular energies is performed first, neglecting the small dependence of transmission on perpendicular energy and noting that $\partial f_0/\partial \varepsilon_F = -\partial f_0/\partial \varepsilon_\perp$, so that we are left with simply the Fermi distribution $f_0[(\varepsilon_\parallel - \varepsilon_F)/kT]$.

We obtain the conductivity

$$\frac{1}{\rho_c} = \left.\frac{\partial J}{\partial V}\right|_{V=0} = \frac{e^2 m_\perp E_0}{2\pi^2\hbar^3}\langle Tr\rangle, \quad (2)$$

with $\langle Tr\rangle$ the remarkably simple and appropriate integral over $\varepsilon_\parallel$

$$\langle Tr\rangle = \frac{1}{E_0}\int_0^\infty d\varepsilon_\parallel Tr(\varepsilon_\parallel) f_0[(\varepsilon_\parallel - \varepsilon_F)/kT]. \quad (3)$$

$E_0$ is the corresponding integral without the $Tr(\varepsilon_\parallel)$ factor; at $T = 0$ it is equal to $\varepsilon_F$. This would essentially be the

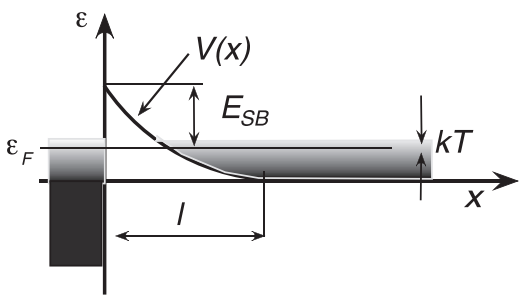


FIG. 1. An energy-level diagram for a metal, on the left, with states filled to the Fermi energy $\varepsilon_F$, and a degenerately doped semiconductor (n-type), on the right, with the same $\varepsilon_F$. A Schottky barrier has arisen of height $E_{SB}$ above the Fermi energy, with a depletion region of thickness $l$.

a)Electronic mail: walt@stanford.edu

 

Richardson equation if we took $\langle Tr\rangle = 1$ for energies above a large Schottky barrier and as zero for energies below. In the prefactor in Eq. (2), $e^2 m_\perp/(2\pi^2\hbar^3)$ is $162\times10^8$ amps/eV volt cm$^2$ (or reciprocal eV Ω cm$^2$), to be multiplied by $m_\perp/m$, equal in silicon to $\sqrt{0.19\times0.98}$ for each of the four transverse valleys for (100) interfaces. At low temperatures $\langle Tr\rangle$ becomes simply $(1/\varepsilon_F)\int_0^{\varepsilon_F} Tr(\varepsilon)d\varepsilon$, but here we consider room temperature and evaluate $\langle Tr\rangle$ numerically.

As usual, we take the depletion approximation for the potential to the right of the interface in Fig. 1 as

$$V(x) = (E_{SB}+\varepsilon_F)(x-l)^2/l^2, \tag{4}$$

measured from the conduction-band minimum (for small applied voltages), with $l=\sqrt{\epsilon_s(E_{SB}+\varepsilon_F)/(2\pi e^2 N_d)}$ from Poisson's equation, where $N_d$ is the donor concentration and $\epsilon_s = 12$ is the relative dielectric constant for silicon (in SI units $4\pi/\epsilon_s$ becomes $1/(\epsilon_0\epsilon_s)$). This form is appropriate at least in the region near the interface where there are few carriers. We also made an evaluation using a more appropriate Fermi-Thomas approximation where the conduction band minimum was below the Fermi energy but found that it made only a small difference so we continued with the depletion approximation (see Eq. (4)).

We use an effective-mass approximation as did Padovani and Stratton[9] but here with longitudinal and transverse masses appropriate to the conduction bands in silicon rather than being isotropic. It is also important to treat correctly the transition to the metal with a different effective-mass. Zhu and Kroemer[14] have shown that the traditional matching of $\psi$ and $(1/m^*)\partial\psi/\partial x$ is not correct and that one must match $(1/\sqrt{m^*})\psi$ and $(1/\sqrt{m^*})\partial\psi/\partial x$. Further, we have shown[15] that the incorrect matching yields opposite shifts from mass differences, relative to correct matching. While Zhu and Kroemer[14] were able to determine the correct matching by using a tight-binding representation of the bands; here we use that same tight-binding representation for the entire calculation not just the interface matching conditions.

In this approach, the wavefunction of the electron is written as a sum of planar wavefunctions $|n\rangle$ of energy $\varepsilon_n$ for the n*th* atomic plane, $|\psi\rangle = \sum_n u_n|n\rangle$, and a variational calculation yields an equation for the $u_n$

$$\varepsilon_n u_n - V_{n,n+1}u_{n+1} - V_{n-1,n}u_{n-1} = \varepsilon u_n, \tag{5}$$

with $-V_{n,n+1}$ the coupling between adjacent plane states. These simplest tight-binding bands in the semiconductor are given by $\varepsilon_k = \varepsilon_n - 2V\cos(ks)$ with $\varepsilon_n = 2V$ if $\varepsilon_k$ is measured from the conduction band minimum, and we choose $V$ for the semiconductor as $V_s = 10.89$ eV to give the light electron mass of 0.19 in silicon with $s = 1.36$ Å as the interplanar distance in (100) silicon. If we were to let $s$ be arbitrarily small, this would lead to the effective-mass Schrödinger equation, but we retain $s$ as the interplanar spacing. Our Eq. (5) will actually incorporate the most important aspect of band nonparabolicity, not included in effective-mass theory, i.e., $\varepsilon_k$ drops below the parabolic curve, as do the real bands, but becomes exactly effective-mass theory at low energies.

We also use this form (Eq. (5)) with $V_m = 3.30$ eV for aluminum as an example metal, with the (100) interplanar spacing $s$ of 2.02 Å, chosen to give the Fermi velocity in aluminum ($\hbar k_F/m = 2.03\times10^6$ m/s) at midband ($\cos(ks)=0$), and we choose the $\varepsilon_n$ in the metal equal to the $\varepsilon_F$ of Fig. 1. Near the interface in silicon $\varepsilon_n$ is equal to $2V_s$ plus the $V(x)$ in Eq. (4) with $x = sn$.

Our approach for calculating the transmission through the interface is to assume some value for $\varepsilon_F$ so that we can calculate the $\varepsilon_n$ from Eq. (4). We then construct a transmitted wave, $\exp(-ik_F sn)$, in the metal for some $\varepsilon$ and obtain each successive $u_{n+1}$ from Eq. (5), through the interface and into the silicon, with the appropriate $\varepsilon_n$ on each plane, into the region beyond the shifts. For the interface coupling $V_{0,1}$ we use $\sqrt{V_m V_s}$ following Zhu and Kroemer.[14] We use the resulting coefficients to determine the incident and reflected amplitudes in the silicon and the corresponding transmission just as in Ref. 15. We calculate $\langle Tr\rangle$ from Eq. (3) for $T = 300$ K. We calculate the electron density in the bulk silicon, taken as $N_d = \int n(\varepsilon) f_0[(\varepsilon-\varepsilon_F)/kT]d\varepsilon$, for our initial choice of $\varepsilon_F$ for that temperature.

This is performed first for the four transverse valleys in silicon. The same calculation for the two longitudinal valleys with the $0.98m$ parallel mass and small perpendicular mass gives a negligible contribution to the conductivity in Eq. (2). Thus we may multiply the one-valley contribution to the conductivity from Eq. (2) by four and take the reciprocal to obtain the interface resistivity. This is plotted as a function of doping density $N_d$ for a range of Schottky-barrier heights in Fig. 2. We shall see that changing the metal has very little effect on the transmission in our effective-mass approximation and so have included data on interfaces with PtSi and NiSi. Increasing the temperature lowered the curves at low doping. Raising $T$ from 300 K to 400 K lowered the 0.4 eV curve close to the room temperature curve shown for $E_{SB} = 0.3$ eV, while for doping above $5\times10^{19}$ cm$^{-3}$ there is little difference between 0.4 eV curves.

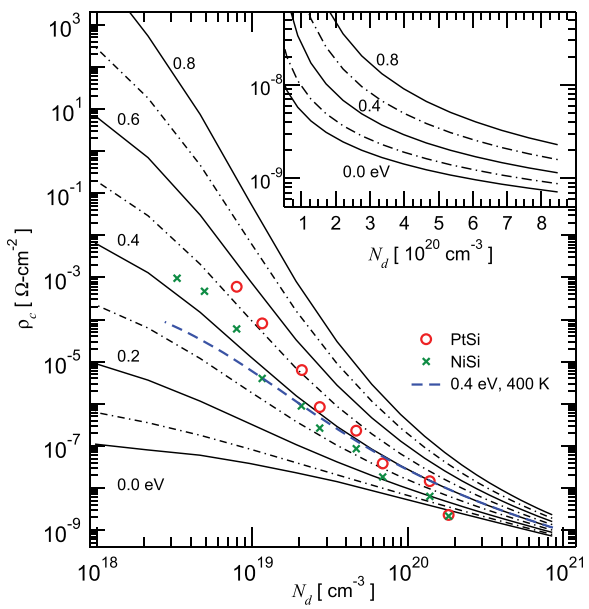


FIG. 2. The specific interface resistivity $\rho_c$ as a function of doping at room temperature (300 K), calculated directly from Eqs. (2) and (3) for several Schottky barrier heights in steps of 0.1 eV (0.2 eV for the inset). Experimental values for PtSi and NiSi are from Stavitski.[16]

Yu[10] used the Padovani and Stratton[9] approach to obtain theoretical curves which were closer to the data he collected than our results but needed an assumed isotropic effective-mass of 0.5 m (Fig. 7 in Ref. 10) We regard ours as a more accurate effective-mass solution, with no adjustable parameters other than $E_{SB}$. In order to better understand these results, it is helpful to approximate some aspects of the analysis.

There are two central features determining $\langle Tr \rangle$. The first is the limited transmission even without any Schottky barrier due to the very different character of the wavefunctions in the metal and those in the semiconductor being matched at the interface. This effect is easily estimated for effective-mass theory for which the transmission for a longitudinal wavenumber $k_{\|}$ in the semiconductor and $k_F^m$, very much larger in the metal (with negligible change over the energy range of importance), is[15]

$$Tr = 4k_{\|}k_F^m/(k_{\|} + k_F^m)^2 \approx 4k_{\|}/k_F^m. \tag{6}$$

At low temperatures the average of this as in Eq. (3) is $8k_F^{\|}/(3k_F^m)$, where $k_F^{\|}$ is the Fermi wavenumber in the direction of current flow in the semiconductor. For the transverse valleys in silicon, with doping of $10^{20}\,\mathrm{cm}^{-3}$, this factor would be 0.094. It is interesting that this is such a large reduction. Padovani and Stratton[9] used the WKB approximation, which treats the variation of the potential with position as small over distances of the order of the electron wavelength. The consequence of this assumption is finding that when the potential increases, it simply slows the electron just as a slowly varying refractive index slows light, but does not reflect it. The electron wavelength is 10.5 nm at the Fermi energy at $10^{20}\,\mathrm{cm}^{-3}$ doping of silicon, so the metal interface is in fact very abrupt on this scale, and the transmission we indicated of 0.094 without any Schottky barrier is appropriate and missed by WKB. This low transmission is inherent to a semiconductor-metal interface and is absent from the earlier theory.

The second feature of the transmission is that with a Schottky barrier, electrons may tunnel through the barrier, which they can do for high doping when the barrier is thin. For this feature the WKB approximation used in the earlier theory should be more appropriate, with a wavefunction taken to vary as $\exp[-\int \mu(x)\,dx]$ where the kinetic energy is negative. We may estimate $\mu(x)$ for electrons at the Fermi energy, taking $V(x)$ as linear in $x$ through the tunneling region, to obtain an additional factor in the transmission as

$$\langle Tr \rangle \approx \frac{8k_F^s}{3k_F^m} \exp\left[-\sqrt{\frac{m_{\|}\epsilon_s(E_{SB}+E_F)}{\pi\hbar^2 e^2 N_d}} \times (\sqrt{E_{SB}+E_F} - \sqrt{E_F})\right]. \tag{7}$$

The main point in making these approximations is to make more apparent the role of the different parameters of the system, which are hidden in the full numerical calculation leading to Fig. 2 and in the expression of Padovani and Stratton which contain many secondary parameters.[9] However, we may also note that only if one neglects $E_F$ in comparison to $E_{SB}$ in Eq. (7) we do obtain the form $\exp[-E_{SB}/E_{00}]$ of all the expressions for current given by Padovani and Stratton,[9] so they have made that approximation presumably just before their Eq. (14). It turns out not to be such a good approximation: For $E_{SB} = 0.7\,\mathrm{eV}$ and $N_d = 10^{20}\,\mathrm{cm}^{-3}$ the exponential in Eq. (7) is smaller by a factor of 0.264 than $\exp[\sqrt{m_{\|}\epsilon_s/(\pi\hbar^2 e^2 N_d)}\,E_{SB}]$.

We may also note that temperature does not (explicitly) enter Eq. (7). The lack of temperature dependence is appropriate at high doping where the barrier is thin, and tunneling dominates (see Fig. 2). Equation (7) can also be used to see the effect of crystal orientation on the resistivity. For a (111) interface the only changes are from the $\sqrt{m_{\|}}$ factor, increasing $\rho_c$, but now all six valleys contribute, leading to a very small net change, as we confirmed numerically. There is also a small decrease in the $m_{\perp}$ in Eq. (2) which increases $\rho_c$ slightly. We note, in addition, that the only place where the properties of the metal enter is in a factor of $1/k_F^m$ in Eq. (7). The Fermi wavenumber scarcely varies by more than a factor of two over the simple metals and would be similar in the silicides, and this tells us that at least in effective-mass theory the predicted interface resistivities are very insensitive to the metal. For that reason the more recent data from silicides was included in Fig. 2. We confirmed this insensitivity in the full calculation, setting $E_{SB} = 0.4\,\mathrm{eV}$, $N_d = 10^{19}/\mathrm{cm}^3$ and varying $\pi/2 - 0.5 < k_F s < \pi/2 + 0.5$ on the metal side; the calculated $\rho_c$ was approximately proportional to $k_F s$ though with a slope 20% larger. In a separate study, we have performed beyond effective-mass theory to include additional bands and find more significant differences between metals which we plan to discuss in a separate communication.

Returning to the full formulation (Eqs. (2) and (3)), we may note that it presents a clearer picture of the nature of the conduction than is usually available. Except for numerical factors the conductance arises entirely from the integral of $Tr(\varepsilon) \times f_0(\varepsilon)$ in Eq. (3), and the distribution across energy is proportional to that dimensionless product. We plot that product and the individual factors versus the energy measured from the Fermi energy in Fig. 3 at four different doping densities, all for $E_{SB} = 0.4\,\mathrm{eV}$, all obtained directly from the calculation of the corresponding curve in Fig. 2. We see that the transmission rises from zero at the conduction-band minimum quite smoothly through the top of the Schottky barrier, while $f_0$ drops from one to zero centered around $\varepsilon_F$.

In Fig. 3, at low doping ($10^{17}\,\mathrm{cm}^{-3}$), where the barriers are thick, the transmitted electrons are from energies close to the barrier top, well above the conduction band minimum $\varepsilon_c$, and would usually be described as *thermionic emission current*, though half of the current came from electrons *technically tunneling*. Going to $10^{18}\,\mathrm{cm}^{-3}$, the $\varepsilon_c$ drops with respect to the Fermi energy. The peak contribution is still near the barrier top but with a much smaller portion going over the barrier, a circumstance frequently called *thermionic field emission*. Further increasing the doping to $10^{19}\,\mathrm{cm}^{-3}$ firmly shifts the peak contributions to below the barrier, i.e., *tunneling current*, as expected. We can see that at very high doping of $10^{20}\,\mathrm{cm}^{-3}$, for which the barrier is very thin, the current is almost entirely from states far below the barrier peak shown at 0.4 eV in Fig. 3.

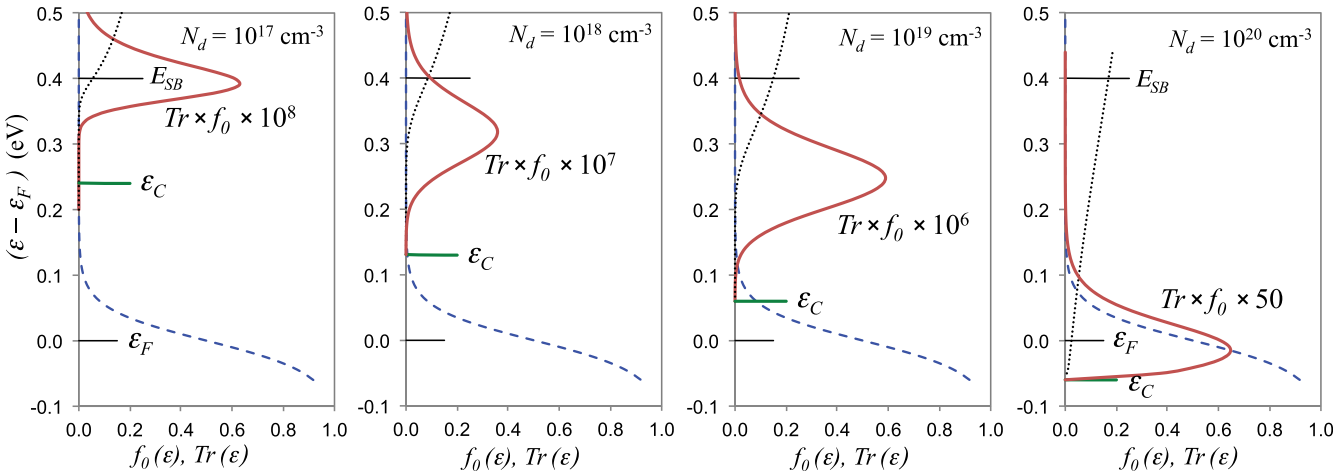


FIG. 3. For four doping densities and zero bias: the dashed lines show the Fermi distribution, the dotted lines the transmission $Tr(\varepsilon)$. The full lines show the product $Tr(\varepsilon) \times f_0$; the current is proportional to the area underneath the peak.

Through the whole process, the size of the peak has continued to increase drastically; note the scale factors differ by $2 \times 10^6$ to make the peaks visible. We see that there is only a single peak, moving down with increasing doping, and never multiple peaks. If the transmission were discontinuous at the top of the barrier as sometimes assumed, then there *would* always be a second peak above the barrier, but we see from Fig. 3 that the transmission coefficient is a smooth continuous function. Also, there is no sharp distinction between the three contributions to current; they meld smoothly from one to the other. This scenario can easily be missed when one makes different approximations in treating the different regimes, as justified as those approximations may be in each case. Moreover, in contrast to classical physics, Fig. 3 shows that even above the barrier the transmission $Tr(\varepsilon)$ depends on the thickness and shape of the barrier, despite the barrier height being the same in each case.

[1]F. Braun, Ann. Phys. **229**, 556 (1875).
[2]W. Schottky, Naturwiss. **26**(52), 843 (1938).
[3]R. T. Tung, Mater. Sci. Eng. R. **35**, 1–138 (2001); W. Mönch, *Electronic Properties of Semiconductor Interfaces* (Springer, Heidelberg, 2007); L. J. Brillson, *Surfaces and Interfaces of Electronic Materials* (Wiley-VCH Verlag GmbH & Co. KGaA, Weinheim, Germany, 2010).
[4]International Technology Roadmap for Semiconductors, 2011.
[5]D. Connelly, C. Faulkner, P. A. Clifton, and D. E. Grupp, Appl. Phys. Lett. **88**, 012105 (2006).
[6]B. E. Coss, W.-Y. Loh, R. M. Wallace, J. Kim, P. Majhi, and R. Jammy, Appl. Phys. Lett. **95**, 222105 (2009).
[7]Z. Zhang, F. Pagette, C. D'Emic, B. Yang, C. Lavoie, A. Ray, Y. Zhu, M. Hopstaken, S. Maurer, C. Murray *et al.*, IEEE Electron Device Lett. **31**, 731 (2010).
[8]A. Agrawal, N. Shukla, K. Ahmed, and S. Datta, Appl. Phys. Lett. **101**, 042108 (2012).
[9]F. A. Padovani and R. Stratton, Solid-State Electron. **9**, 695 (1966).
[10]A. Y. C. Yu, Solid-State Electron. **13**, 239 (1970).
[11]C. R. Crowell and S. M. Sze, J. Appl. Phys. **37**, 2683 (1966).
[12]C. Y. Chang, Y. K. Fang, and S. M. Sze, Solid-State Electron. **14**, 541 (1971).
[13]K. K. Ng and R. Liu, IEEE Trans. Electron Devices **37**, 1535 (1990).
[14]Q.-G. Zhu and H. Kroemer, Phys. Rev. B **27**, 3519 (1983).
[15]W. A. Harrison, J. Appl. Phys. **110**, 113715 (2011).
[16]N. Stavitski, M. J. H. van Dal, A. Lauwers, C. Vrancken, A. Y. Kovalgin, and R. A. M. Wolters, IEEE Electron Device Lett. **29**, 378 (2008).